Hindawi
Applied Bionics and Biomechanics
Volume 2023, Article ID 5722499, 14 pages
https://doi.org/10.1155/2023/5722499

Research Article

Design and Analysis of a Hemispherical Parallel Mechanism for Forearm–Wrist Rehabilitation

Shuang Li, Zhanli Wang, Zaixiang Pang, Moyao Gao, and Zhifeng Duan

School of Mechatronic Engineering, Changchun University of Technology, Changchun 130012, China

Correspondence should be addressed to Zhanli Wang; wangzl@ccut.edu.cn

Received 13 November 2022; Revised 9 February 2023; Accepted 16 February 2023; Published 13 March 2023

Academic Editor: Wen-Ming Chen

This paper presents a bionic cable-driven mechanism to simulate the motion of human wrist which is suitable for human forearm–wrist rehabilitation. It fulfills workspace of the human forearm–wrist and it can train the joint in active and passive. With three degrees of freedom, it completes the supination/pronation of the forearm, the radial/ulnar deviation, and flexion/extension of the wrist. In addition to the movement of single degree of freedom of the forearm–wrist, it can also complete circumduction of the wrist. The mechanism consists of revolving platform, parallel mechanism, supporting mechanism, and movable table. Especially, in the parallel mechanism, a spring is added between the fixed and moving platform, and the moving platform is designed in the shape of a hemispherical shell. Utilizing the resilient properties of the extension spring and the support of the hemispherical shell, the problem of slack in the cable is solved in this mechanism. Since the spring is a passive component and cannot be calculated directly, a method combining kinematics and statics is proposed to calculate the relationship between the pose of the moving platform and the cable. Meanwhile, the kinematics, statics, and workspace solution of the mechanism are derived. Then, the simulation results demonstrate the accurateness and feasibility of the inverse kinematics and workspace derivation of the mechanism. Finally, the experiments are analyzed to verify the mechanism suitable for forearm–wrist rehabilitation tasks.

1. Introduction

With aging, stroke, Parkinson's disease, accidents, and other factors will have varying degrees of damage on the upper limbs of the human [1, 2]. The patients not only suffer mentally and physically, but also work and daily life. Existing research shows that the treatment of upper limb timely and correctly has a positive effect on their upper limb function. In traditional rehabilitation progress, the patient's upper limb is trained passively by therapists who use different treatment methods. This treatment is monotonous, repetitive, and less efficient which is difficult to ensure the stability and continuity of rehabilitation training. Therefore, it is necessary to find better means to solve this problem, and the method of using rehabilitation devices has emerged timely [3, 4]. It not only improves the treatment effect and reduces the workload of the therapist, but also can specially train the patient's joints to speed up the patient's recovery.

In recent years, many robotic devices for upper limb rehabilitation are proliferating, such as MIT-Manus [5], CAREX [6, 7], ARM guide [8], MIME [9], and Armeo Spring [10]. However, in the area of rehabilitation devices for the upper limb, there is a small quantity of aiming at training the wrist joint's devices. The wrist joint plays an important role in people's daily activities including lifting, pulling, pushing, and other movements. The performance of the wrist significantly affects the function of the hand [11]. At present, wrist joint is a passive joint mostly in some upper limb rehabilitation devices, which requires patients to exercise their wrist joints actively by themselves. Therefore, it is significant to develop rehabilitation devices that cover the completed workspace of human forearm–wrist and train the joint in active and passive.

In addition to upper limb rehabilitation devices that might include some wrist movements, researchers have conducted research on rehabilitation devices about training

forearm–wrist with three degrees of freedom (DoFs) for the rehabilitation, such as Ricewrist, RiceWrist-S, MAHI EXO II, and WRES. The Ricewrist robotic device is composed of a parallel mechanism and elastic actuators, which is compact, has low-friction, and is backlash-free, with high manipulability in the workspace of interest. To ensure that the device is aligned with the rotation axis of the wrist, it is difficult to be don/doff [12]. The RiceWrist-S is modified on the base of Ricewrist robotic device provided lower inertia, higher torque output capabilities, and a more robust system [13]. The MAHI EXO II is a five DoFs haptic arm exoskeleton for rehabilitation [14]. The device provides kinesthetic feedback to the joints of the operator's lower arm and wrist and it is an updated design based on the work of MAHI [15]. The WRES adopts a tendon cable transmission for three joints. It is driven by cables and more suitable for rehabilitation devices than rigid parallel mechanisms [16]. Their structures can only be used for rehabilitation training on one side, and they cannot be applied to two hands without changing the structure, nor can they perform compound orbiting movements around the wrist joints [17, 18]. Although WRES has three DoFs that can be used for both left and right hands, it cannot perform wrist circumduction movements.

In addition to the movement of a single DoF, the rehabilitation exercise of the wrist joint can also carry out the wrist circumduction—a full circular motion made by the wrist. The circumduction is the proximal end of the bone that rotates in situ, and the distal end makes a circular motion. The trajectory of the entire bone movement is conical [11]. Based on rehabilitation theory, it is known that the wrist circumduction is one of the compound movement, and compound movement can better recover the wrist joint of stroke patients.

Therefore, this paper develops and validates a three DoFs mechanism for rehabilitation of the forearm–wrist. The mechanism is simple, light, and flexible which will not cause secondary damage to the patients. The proposed mechanism is mainly composed of a revolving platform, a parallel mechanism, and a supporting mechanism. The revolving platform completes the supination/pronation (S/P) of the forearm. The movement of the wrist includes the radial/ulnar (R/U) deviation and flexion/extension (F/E) by the parallel mechanism. The supporting mechanism plays a supporting role in process of rehabilitation. In this paper, the work focuses on the parallel mechanism. Parallel mechanisms are widely used in the field of rehabilitation robots. Rastegarpanah et al. [19] studies a six DoFs parallel mechanism for lower limb rehabilitation robot. Cafolla et al. [20] introduce a cable-driven parallel mechanism which is used for upper and lower limb for the assistance of patients in rehabilitation exercising. Gao et al. [21] design a cable-driven parallel mechanism with a spring spine which is a humanoid neck robot. Generally, a cable-driven parallel mechanism with two DoFs motion of pitch and roll is driven by three actuators and three cables [21, 22]. Owing to the characteristics of unidirectional force of the cable, the cable may be slack when driving the moving platform. To address this problem, a hemispherical shell is designed in the parallel mechanism, which provides reverse tension for the cables to support the entire structure and satisfy the mobility of the forearm–wrist.

At the same time, according to the stretchable nature of the spring, the parallel mechanism uses an extension spring instead of a cable to keep the other two cables under tension when the moveable platform is moving. Adding the spring does not change the DoFs of the mechanism, and the mechanism maintains the original motion. Meanwhile, the spring is driven by the other two cables so that an actuator can be eliminated, therefore the mechanism reduces the cost and weight. The rehabilitation structures designed in this paper can be used for bilateral wrist rehabilitation, respectively. It can not only complete the movement of three DoFs but also complete the wrist circumduction. In terms of alignment, the center is coincident with the capitate by adjusting the external slider. Even if the axis does not coincide with the capitate, it will not cause secondary injury to the patient's wrist joint; it will affect the range of motion of the joint due to the uniqueness of the designed structure. The mechanism proposed in this paper can train the forearm–wrist in active and passive. At the same time, it will apply to ankle rehabilitation.

This paper focuses on developing a rehabilitation mechanism that imitates the movement in the human forearm–wrist. A particular aim is to propose an original and novel idea of the parallel mechanism. The parallel mechanism adds spring to solve the problem of cable slack and decreases an actuator without changing the mobility. To investigate the performance of the developed mechanisms by measuring the physiological motion space of the forearm–wrist and by evaluating the accurateness of the performed calculations.

2. Mechanical Design

2.1. Measurement of Forearm and Wrist. Wrist joint is a complex joint composed of multiple joints, including the radio–wrist joint, intercarpal joint, and carpal–metacarpal joint. When the human wrist is moving, the head of the capitate is the axis of rotation for wrist joint [11]. The movement of the wrist includes the F/E and R/U deviation, wrist circumduction, and the S/P of the forearm, as shown in Figure 1.

To improve the movement of forearm–wrist of people with stroke and disablility, the first aim is to develop a novel mechanism for rehabilitation that accurately replicates the human forearm–wrist joint movement. A forearm–wrist mechanism (FWM) used for forearm–wrist rehabilitation should possess three DoFs for F/E and R/U deviation, S/P, and circumduction movement which is cover the whole workspace of the forearm and wrist. As rehabilitation equipment, FWM can be used independently or installed at the terminal of upper limb rehabilitation mechanism.

In order to the joint ROM of the mechanism to satisfy the physiological motion space (PMS) of the forearm and wrist, it is significant to measure the PMS of the movement of the forearm and wrist joint. The experimental platform is designed to measure the PMS during autonomous motions of the forearm and wrist.

(a) (b) (c) (d)

Figure 1: The movement of the forearm and wrist. (a) F/E of the wrist. (b) R/U deviation of the wrist. (c) S/P of the forearm. (d) Wrist circumduction.

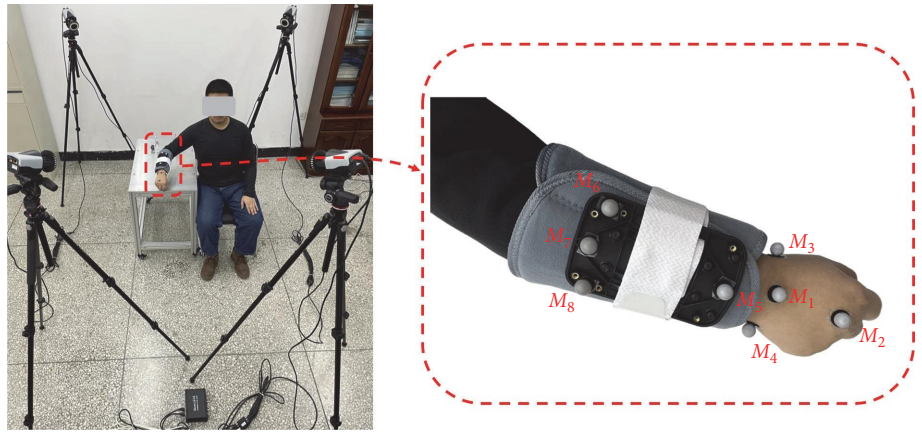

(a) (b)

Figure 2: Measurement experiments of physiological motion space. (a) Overall equipment. (b) Placed reflective markers.

Figure 2(a) shows the setup of the experiment. The experimental platform predominantly consists of the Qualisys Track Manager (QTM) system and reflective markers. Using a QTM camera system, typical human forearm and wrist kinematics for motion were measured at 100 Hz as a benchmark [23]. Reflective markers were placed on the anterior and posterior regions of the wrist of individuals, as shown in Figure 2(b).

The marker M_1 was placed on the capitate of the wrist joint [24]. The markers M_2–M_5 and M_6–M_8, which were placed on the forearm and hand, form reference frame to label the attitudes of the forearm and wrist. In the experiments of measurement, the forearm and wrist completed the full range of autonomous movement. During the experiments, the participants moved the forearm and wrist maximally. The participants should fulfill F/E, R/U deviation movement of the wrist joint, and S/P of the forearm and wrist circumduction, respectively. For each motion, the participants completed it three to five times within 15 s. After completing a group of motions, there was a short rest period. Data collection for the next set of motions was performed after 1 min of rest. The difference in the exercise period was because the two experiments are carried out by people actively exercising, therefore the exercise period was different, but the trend was the same.

The data are recorded by the infrared cameras every time and saved by the software. The obtained data are imported into the MATLAB software for data processing, and the result is shown in Figure 3. Every period of every line in Figure 3(a) shows that the participant completes the flexion movement first and then extension. As Figure 3(a), Figure 3(b) shows that the participants complete the radial deviation first and ulnar deviation next, and Figure 3(c) shows the supination and pronation. And five lines illustrate that the five sets of data were collected. According to Figure 3, it is obtained that the maximum angle of flexion is 51.4 and extension is 49.7, radial deviation is 12.33, ulnar deviation is 15.67, supination is 74.6, and pronation is 84.2.

2.2. Design of FWM. According to the characteristics of the movement of the forearm and wrist, an FWM by cable driven for rehabilitation is developed, as shown in Figure 4. It is composed of revolving platform, parallel mechanism, supporting mechanism, and movable table. The parallel mechanism includes a fixed platform (rotational board and frame of hemispherical shell), a moving platform (hemispherical

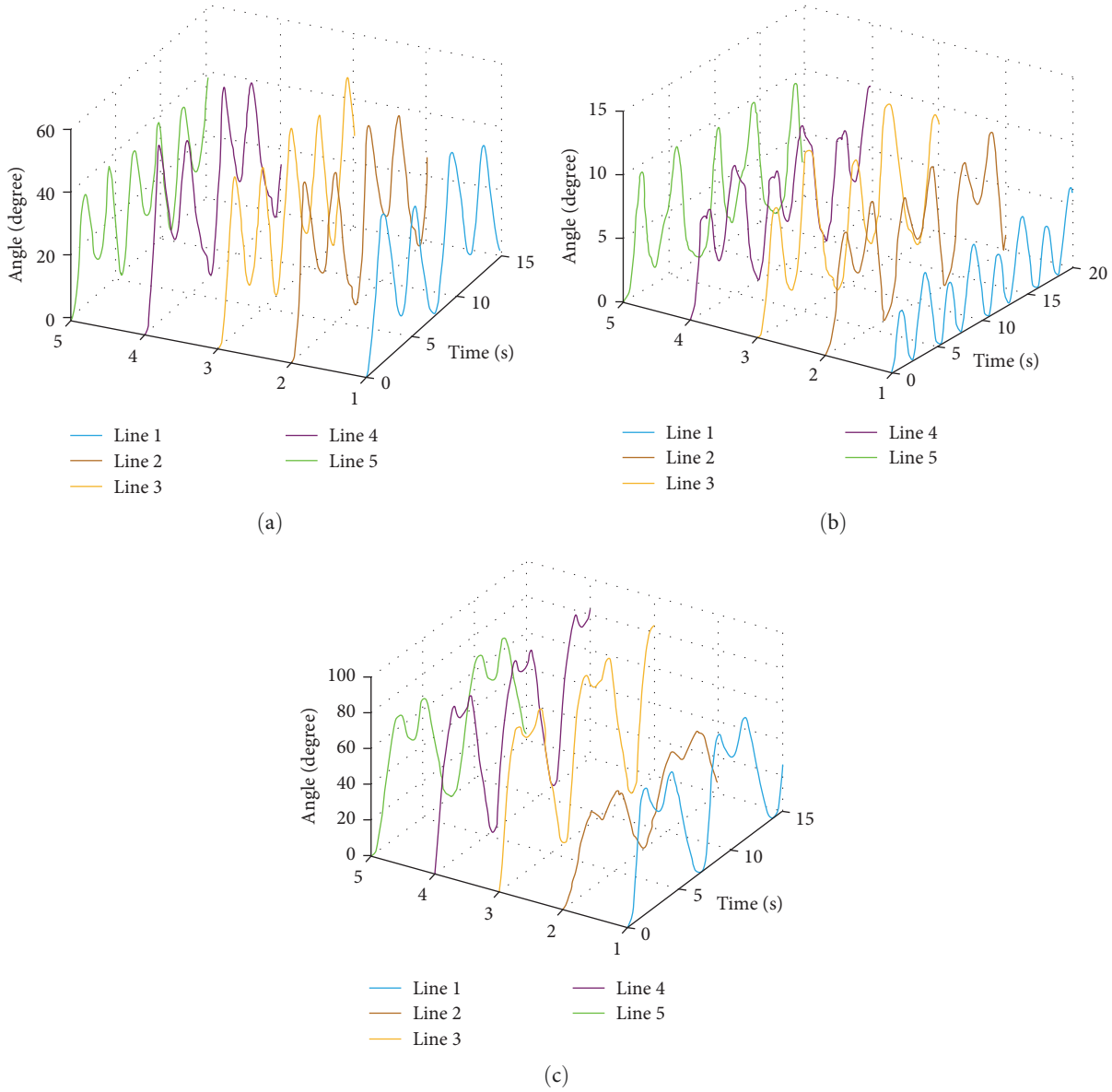

Figure 3: PMS of forearm and wrist joint. (a) F/E. (b) R/U deviation. (c) S/P.

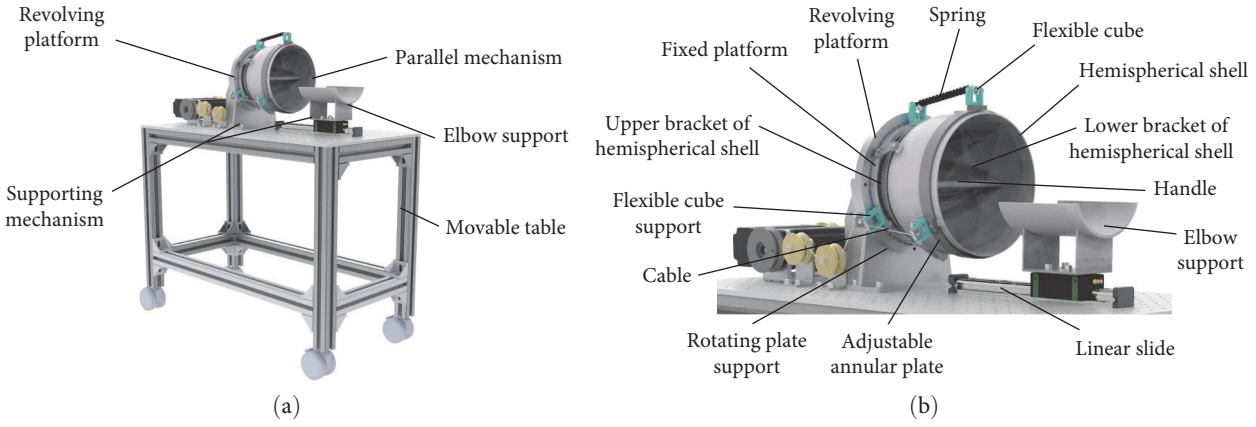

Figure 4: Three-dimensional model of cable-driven mechanism. (a) Oblique side view. (b) Detail view.

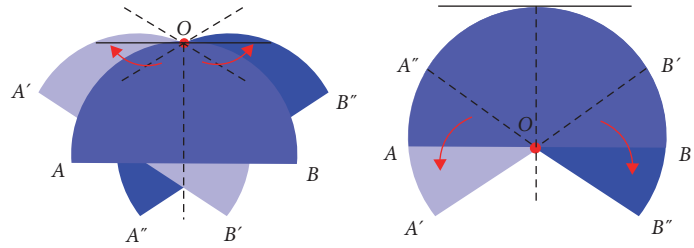

FIGURE 5: The difference between two types of the mechanism. (a) Traditional spherical joint. (b) Hemispherical shell.

shell), two cables, and an extension spring connecting the moving and fixed platform. The fixed platform connects the parallel mechanism by the revolving platform. The end of the cable is reeled by a pully which is connected to a motor, and the other end crosses the rotational board to connect the fixed and moving platform.

Compared with the traditional parallel mechanism which has two DoFs with three moving rods, the parallel mechanism in this paper modifies three moving rods of traditional platform into two cables and one spring and adds a hemispherical shell as a support mechanism for the fixed platform and the moving platform. The reasons for designing the mechanism are as follows: (1) to avoid secondary injury for patients during using the equipment, the cable-driven is used to make the device flexible. (2) Because the cable has the characteristics of unidirectional force, the cable will be slack when is used to drive the moving platform to move. To solve the problem, a spring is added, and a hemispherical shell is designed between the fixed platform and the moving platform. (3) The addition of the spring also eliminates one drive rod, which decreases cost and weight. The parallel mechanism can accomplish the same movement driven by two actuators. This section is focused on the parallel mechanism.

The fixed platform of the parallel mechanism is fixed on the revolving platform, and the parallel mechanism completes the movement of the S/P of the forearm by the rotation of the revolving platform. The moving platform of the parallel mechanism is a hemispherical shell, and the upper half of the hemispherical shell is hollowed out, and its Z-direction movement is fixed by two annular shells so that the hemispherical shell can move in the annular shell. The fixed platform and the moving platform are connected by cables and springs. One end of the cable and the spring are fixed on the fixed platform and the other end are connected with the hemispherical shell through flexible cubes. The flexible cubes are installed on the adjustable annular plate to adjust the distance between the fixed and moving platform which is adapted to the hands of different patients.

In the parallel mechanism, cables 1 and 2 are driven by motors, respectively. The spring is a passive part. By changing the length of the cables, the tension of the spring is changed, and the elongation of the spring is also changed. The parallel mechanism completes the U/R, F/E, and circumduction of the wrist due to the changing cables and spring.

The difference between the parallel mechanism with a hemispherical shell designed in this paper and the traditional spherical joint is that the center of rotation of the motion of the spherical joint is the vertex of the sphere connected to the fixed platform, while the hemispherical shell is the center of the sphere; the schematic diagram is shown in Figure 5. The advantage of this design is that the patient's joint will not be injured during the rehabilitation process when the center of the hemispherical shell is offset from the capitate.

2.3. Mobility Analysis of Parallel Mechanism. In order to better describe and simplify the mobility analysis of FWM, this section will first discuss the parallel mechanism using the screw theory. The branch coordinate system of the parallel mechanism is shown in Figure 6. It consists of a fixed platform $A_1A_2A_3$, a movable platform $B_1B_2B_3$, and three identical UPU branches.

The origin of the branch coordinate system in the i-th branch is located on point O_i. The Z_i-axis' direction is B_1 to A_1 and the X_i-axis' direction is parallel to the B_1 to the perpendicular line of B_2 and B_3. Y_i-axis' direction is defined by the right-hand rule. The D branch uses the same coordinate system with the i-th branch.

According to the screw theory, in the O_i– $X_iY_iZ_i$ system, the kinematic screw axes system of the i-th branch is as follows:

$$\begin{cases} \$_{i1} = (0 \quad 1 \quad 0; 0 \quad 0 \quad 0)^T \\ \$_{i2} = (1 \quad 0 \quad 0; 0 \quad 0 \quad 0)^T \\ \$_{i3} = (0 \quad 0 \quad 0; 0 \quad 0 \quad 1)^T \\ \$_{i4} = (0 \quad 1 \quad 0; 0 \quad 0 \quad l)^T \\ \$_{i5} = (1 \quad 0 \quad 0; 0 \quad 0 \quad l)^T, \end{cases} \tag{1}$$

where the parameter l is the distance between the A_i of the movable platform and B_i of the fixed platform.

Obviously, the constraint screw axes of the i-th branch is as follows:

$$\$_i^r = (1 \quad 0 \quad 0; 0 \quad 0 \quad 0)^T. \tag{2}$$

The kinematic screw axes system of the D branch is as follows:

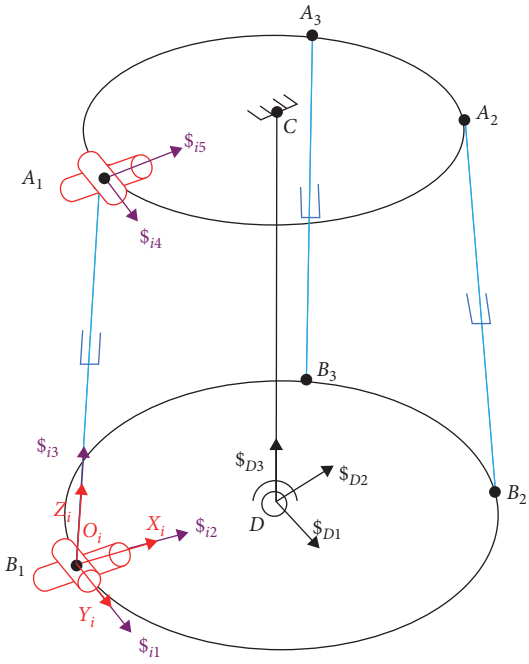

Figure 6: The branch coordinate system of the parallel mechanism.

$$\begin{cases} \$_{D1} = (0 \quad 1 \quad 0; 0 \quad 0 \quad c_1)^T \\ \$_{D2} = (1 \quad 0 \quad 0; 0 \quad 0 \quad -c_2)^T \\ \$_{D3} = (m \quad 0 \quad n; c_2 \quad c_1 \quad 1)^T, \end{cases} \tag{3}$$

where c_1, c_2, m, and n are representations of the twist's parameters in O_i– $X_iY_iZ_i$ system.

The constraint screw axes system of the D branch is as follows:

$$\begin{cases} \$^r_{D1} = (0 \quad 0 \quad 1; c_2 \quad -c_1 \quad -mc_2)^T \\ \$^r_{D2} = \left(1 \quad 0 \quad 0; -\frac{c_2}{m} \quad 0 \quad 0\right)^T \\ \$^r_{D3} = \left(0 \quad 1 \quad 0; 0 \quad 0 \quad -\frac{c_2}{n}\right)^T. \end{cases} \tag{4}$$

Equations (2) and (4) obtain the constraint screw axes system:

$$\begin{cases} \$^r_1 = (1 \quad 0 \quad 0; 0 \quad 0 \quad 0)^T \\ \$^r_2 = (0 \quad 0 \quad 1; c_2 \quad -c_1 \quad -mc_2)^T \\ \$^r_3 = \left(1 \quad 0 \quad 0; -\frac{c_2}{m} \quad 0 \quad 0\right)^T \\ \$^r_4 = \left(0 \quad 1 \quad 0; 0 \quad 0 \quad -\frac{c_2}{n}\right)^T. \end{cases} \tag{5}$$

The reciprocal screw axes of Equation (5) is as follows:

$$\begin{cases} \$^g_1 = (1 \quad 0 \quad 0; 0 \quad 0 \quad -c_2)^T \\ \$^g_2 = (0 \quad 1 \quad 0; 0 \quad 0 \quad -c_1)^T. \end{cases} \tag{6}$$

Hence, the parallel mechanism has two rotational DoFs. However, the FWM consists of a revolving platform and a parallel mechanism. The revolving platform is connected to the fixed platform of the parallel mechanism to satisfy the rotation of the mechanism, which has one rotational DoF. Therefore, the FWM has three rotational DoFs, and it is suitable for patients to achieve the rehabilitation of forearm and wrist.

3. Inverse Kinematics and Statics

3.1. Inverse Kinematics. In the proposed mechanism, the rotation of revolving platform completes the S/P movement of the forearm. If the motor rotation angle is given, the angle of the forearm rotation can be known. But, the movement of the wrist includes the F/E and R/U deviation by the parallel mechanism. Therefore, the inverse kinematics analysis of the parallel mechanism is necessary to calculate the cables length by given the posture of the moving platform of the parallel mechanism. When the cable length changes, the spring will lengthen or shorten like the cable. It is assumed that spring regard as cables and cables do not have stretch and negligible mass.

According to the human anatomica [11], wrist joint is a complex joint composed of multiple joints, including the radio–wrist joint, intercarpal joint, and carpal–metacarpal joint. When the human wrist is moving, the capitate is the rotation center of wrist joint. Hence, the moving platform rotation center O_B coincides with the capitate, and O_B is the center of the hemispherical shell. As shown in Figure 7, the coordinates of A_i $(i = 1, 2, 3)$ donate the connection points of the two cables and a spring on the fixed platform. B_i $(i = 1, 2, 3)$ donate the connection points of the moving platform.

The fixed coordinate frame O_A– $X_AY_AZ_A$ is attached to the fixed platform at point O_A (the center of the fixed platform). The X-axis is along O_AA_2 and Z-axis is

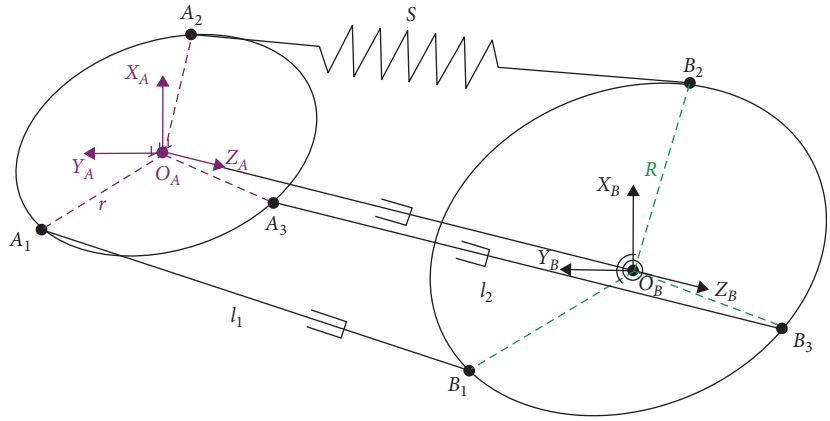

FIGURE 7: The schematic of the parallel mechanism.

perpendicular to the fixed platform. According to the right-hand rule, Y-axis is established. The moving coordinate frame O_B–$X_BY_BZ_B$ is attached to the moving platform at point O_B (the center of the moving platform). The X-axis is along O_BB_2 and Z-axis is perpendicular to the moving platform. Y-axis is determined by the right-hand rule. O_AA_i is in the same direction as the O_BB_i in the initial configuration. The radius of the fixed platform and moving platform are r and R, respectively. The coordinates of A_i in frame O_A–$X_AY_AZ_A$ are described as $A_1 = \left(-r/2, \sqrt{3}/2\ r, 0\right)^T$, $A_2 = (r, 0, 0)^T$, and $A_3 = \left(-r/2, -\sqrt{3}/2\ r, 0\right)^T$. The corresponding coordinates for other ends of the cables B_i in frame O_B–$X_BY_BZ_B$ are $B_1 = \left(-R/2, \sqrt{3}/2\ R, 0\right)^T$, $B_2 = (R, 0, 0)^T$, and $B_3 = \left(-R/2, -\sqrt{3}/2\ R, 0\right)^T$. l_i denotes the cable length between A_i and B_i. The configuration of the moving platform can be described by parameters θ and ϕ, rotate by θ degrees about the X-axis, and rotate by ϕ degrees about the Y-axis, then the rotational matrix is as follows:

$$ {}^A\boldsymbol{R}_B = \begin{bmatrix} t_{11} & t_{12} & t_{13} \\ t_{21} & t_{22} & t_{23} \\ t_{31} & t_{32} & t_{33} \end{bmatrix}, \tag{7} $$

where $t_{11} = \cos\phi$, $t_{12} = \sin\phi\sin\theta$, $t_{13} = \sin\phi\cos\theta$, $t_{21} = 0$, $t_{22} = \cos\theta$, $t_{23} = -\sin\theta$, and $t_{31} = -\sin\phi$, $t_{32} = \cos\phi\sin\theta$, $t_{33} = \cos\phi\cos\theta$.

The cable length l_i is as follows:

$$ l_i = ||\boldsymbol{L}_i|| = ||{}^A\boldsymbol{P}_B + {}^A\boldsymbol{R}_B\boldsymbol{B}_i - \boldsymbol{A}_i, ||,\ i = 1, 2, 3. \tag{8} $$

In fact, the spring is a passive element in the mechanism, which is changed by the force acting on the spring. These forces come from the tension in the cables, and the spring is changed depending on the cables. Therefore, the inverse kinematics cannot be solved directly, and it needs to be combined with the inverse kinematics and statics to obtain the solution.

3.2. Statics. The Jacobian matrix is the key to solve the statics analysis of the mechanism. Thus, it is necessary to calculate the Jacobian matrix of the parallel mechanism before solving the statics.

Equation (8) is given as follows:

$$ l_i^2 = \boldsymbol{L}_i^T\boldsymbol{L}_i\ (i = 1, 2, 3). \tag{9} $$

Taking the time derivation of Equation (9),

$$ l_i\dot{l}_i = \boldsymbol{L}_i^T\left({}^A\dot{\boldsymbol{R}}_B\boldsymbol{B}_i\right), \tag{10} $$

$$ {}^A\dot{\boldsymbol{R}}_B = \boldsymbol{S}(\omega){}^A\boldsymbol{R}_B = {}^A\omega_B \times {}^A\boldsymbol{R}_B, \tag{11} $$

$$ \boldsymbol{S}(\omega) = \begin{bmatrix} 0 & -\omega_z & \omega_y \\ \omega_z & 0 & -\omega_x \\ -\omega_y & \omega_x & 0 \end{bmatrix}, \tag{12} $$

where ${}^A\dot{\boldsymbol{R}}_B$ is the derivation of rotation matrix with respect to time, and $\boldsymbol{S}(\omega)$ is the operator matrix of the angular velocity.

Defining the velocity vector of the joint space as $\dot{\boldsymbol{q}} = \begin{bmatrix} \dot{l}_1 & \dot{l}_2 & \dot{l}_3 \end{bmatrix}^T$ and velocity vector for the moveable platform as $\dot{X} = {}^A\omega_B = \begin{bmatrix} \omega_x & \omega_y & \omega_z \end{bmatrix}^T$, the Jacobian matrix of the parallel mechanism can be calculated as follows:

$$ \boldsymbol{J}_q\dot{\boldsymbol{q}} = \boldsymbol{J}_x\dot{\boldsymbol{X}}, \tag{13} $$

where $\boldsymbol{J}_q$ and $\boldsymbol{J}_x$ are the inverse and direct of the Jacobian matrix, respectively.

$$ \boldsymbol{J}_q = \mathrm{diag}[\, l_1 \quad l_2 \quad l_3\,], \tag{14} $$

$$ \boldsymbol{J}_x = \begin{bmatrix} \left({}^A\boldsymbol{R}_B\boldsymbol{B}_1 \times \boldsymbol{L}_1\right)^T \\ \left({}^A\boldsymbol{R}_B\boldsymbol{B}_2 \times \boldsymbol{L}_2\right)^T \\ \left({}^A\boldsymbol{R}_B\boldsymbol{B}_3 \times \boldsymbol{L}_3\right)^T \end{bmatrix}. \tag{15} $$

According to the force balance relationship of the moving platform, the force of the moving platform is shown in Figure 8, and the statics equation of the mechanism can be obtained as follows:

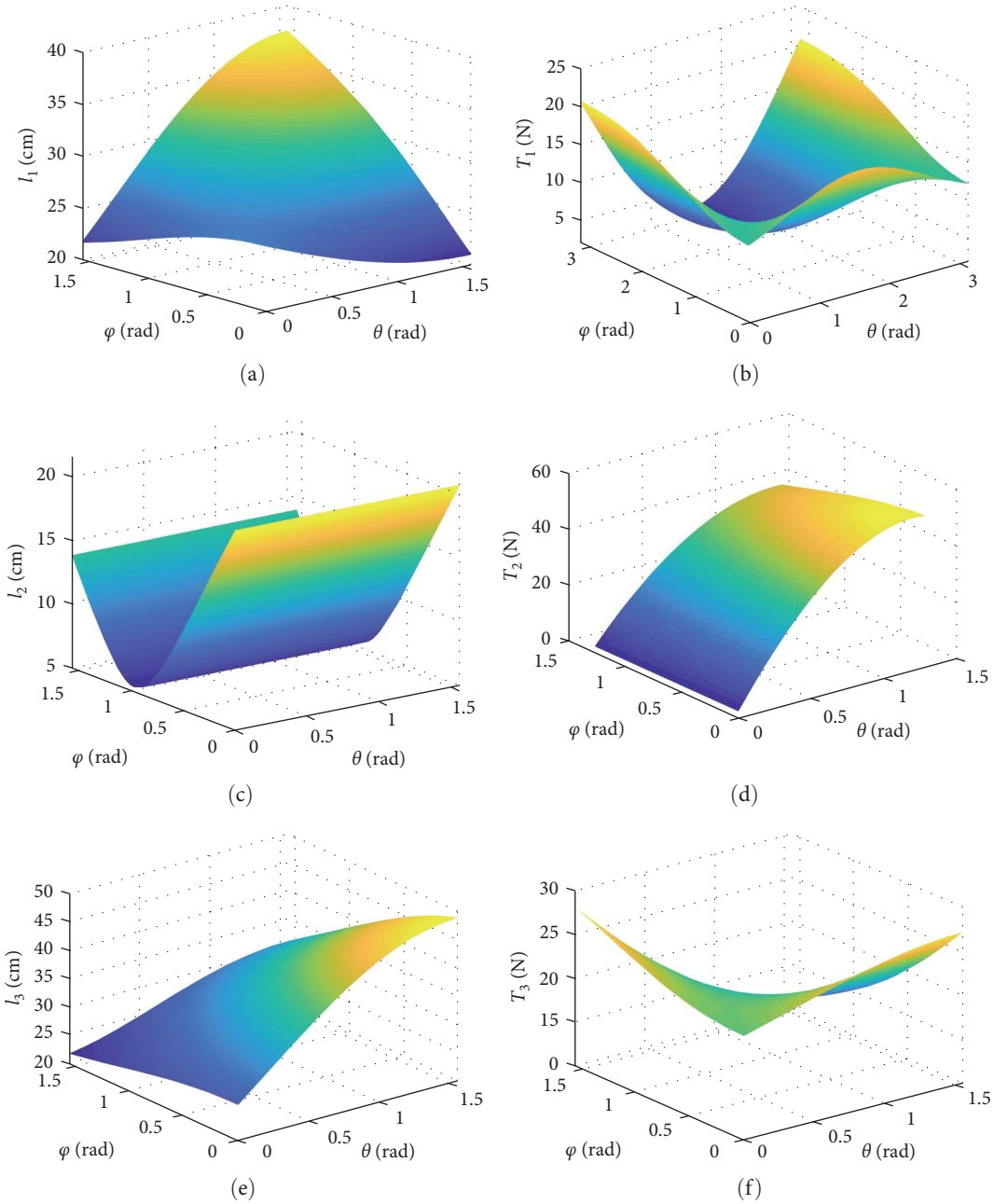

FIGURE 8: Inverse position and statics illustration. (a) The length changes of cable 1. (b) The length changes of spring. (c) The length changes of cable 3. (d) The tension changes of cable 1. (e) The tension changes of spring. (f) The tension changes of cable 3.

$$\boldsymbol{J}^T \boldsymbol{T} = -\boldsymbol{F}_w, \tag{16}$$

where $T = (T_1\ T_2)^T$ is vector of cable's pull, and $\boldsymbol{F}_w$ is twist of external force.

The spring can be regarded as a cable when the Jacobian matrix is being calculated, but when the statics is being calculated, the spring will provide the passive force, so the Jacobian matrix should remove the twist corresponding to the spring in the statics equations. Therefore, the structural matrix of the cable driving part is defined as $\boldsymbol{E} = (\boldsymbol{J}_1\ \boldsymbol{J}_3)^T$, and the structure matrix of the spring is $\boldsymbol{E}_s = \boldsymbol{J}_2{}^T$. When the tension of cable is solving, the force twist of the spring needs to be regarded as the twist of the external force, and then the balance equation of the parallel mechanism is as follows:

$$\boldsymbol{E}\boldsymbol{T} = -(\boldsymbol{F}_w + \boldsymbol{E}_s t_s), \tag{17}$$

where t_s can be obtained using Hooke's law $t_s = k(l - l_0)$, k is the spring constant.

3.3. Simulations. The inverse positions and statics were simulated by MATLAB. Parameters of mechanism for prototype are given as: the radius $r = 0.065$ m, $R = 0.095$ m, the length of $\overrightarrow{O_A O_B} = 0.1044$ m, by varying θ from 0 to $\pi/2$ and ϕ from 0 to $\pi/2$. The relationship between the pose of

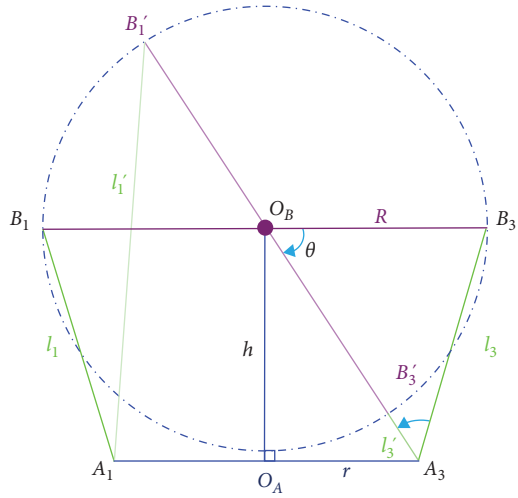

FIGURE 9: Statics illustration.

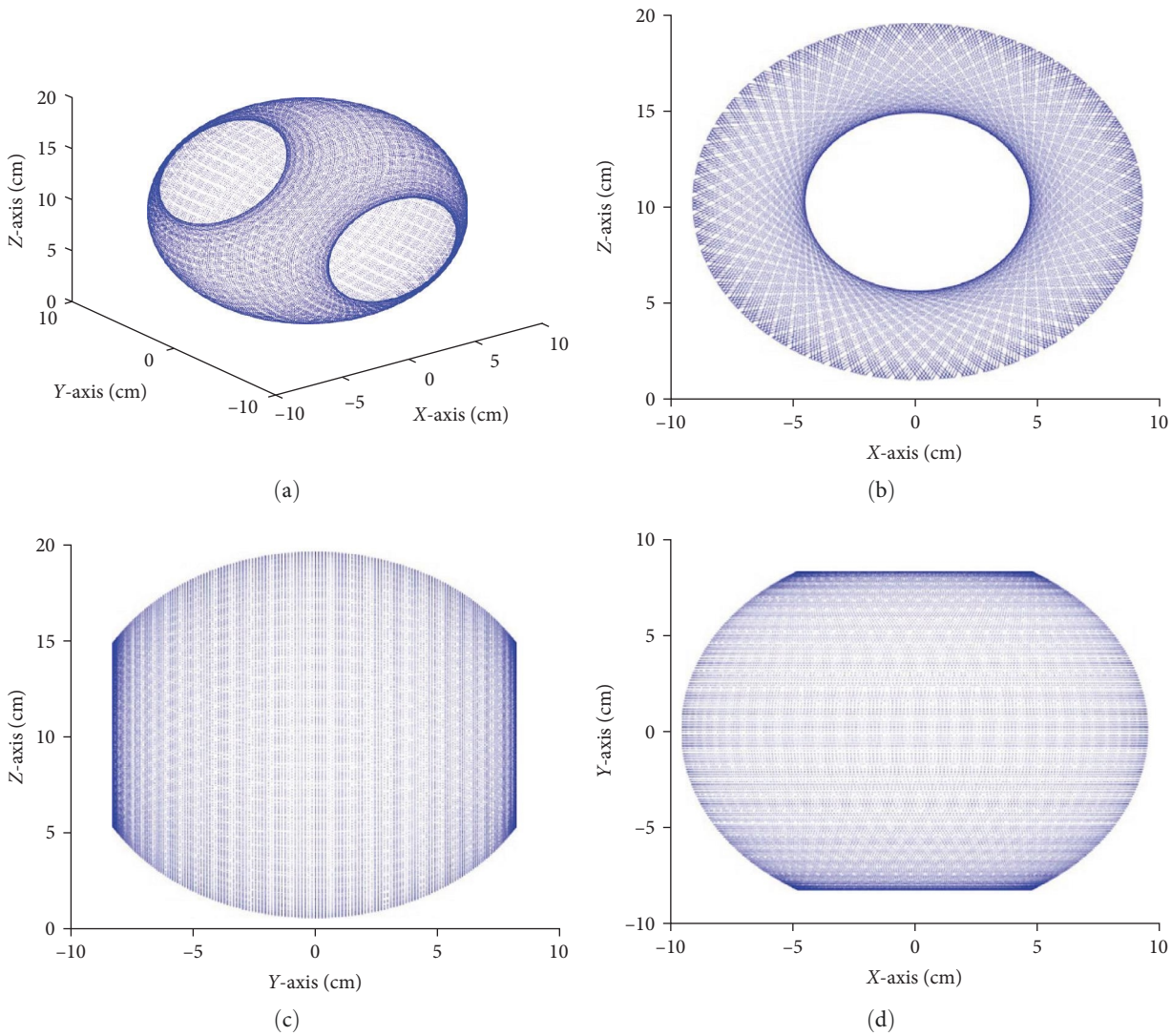

FIGURE 10: The workspace analysis of the FWM. (a) The Cartesian 3D space. (b) X–Z-axis of 2D space. (c) Y–Z-axis of 2D space. (d) X–Y-axis of 2D space.

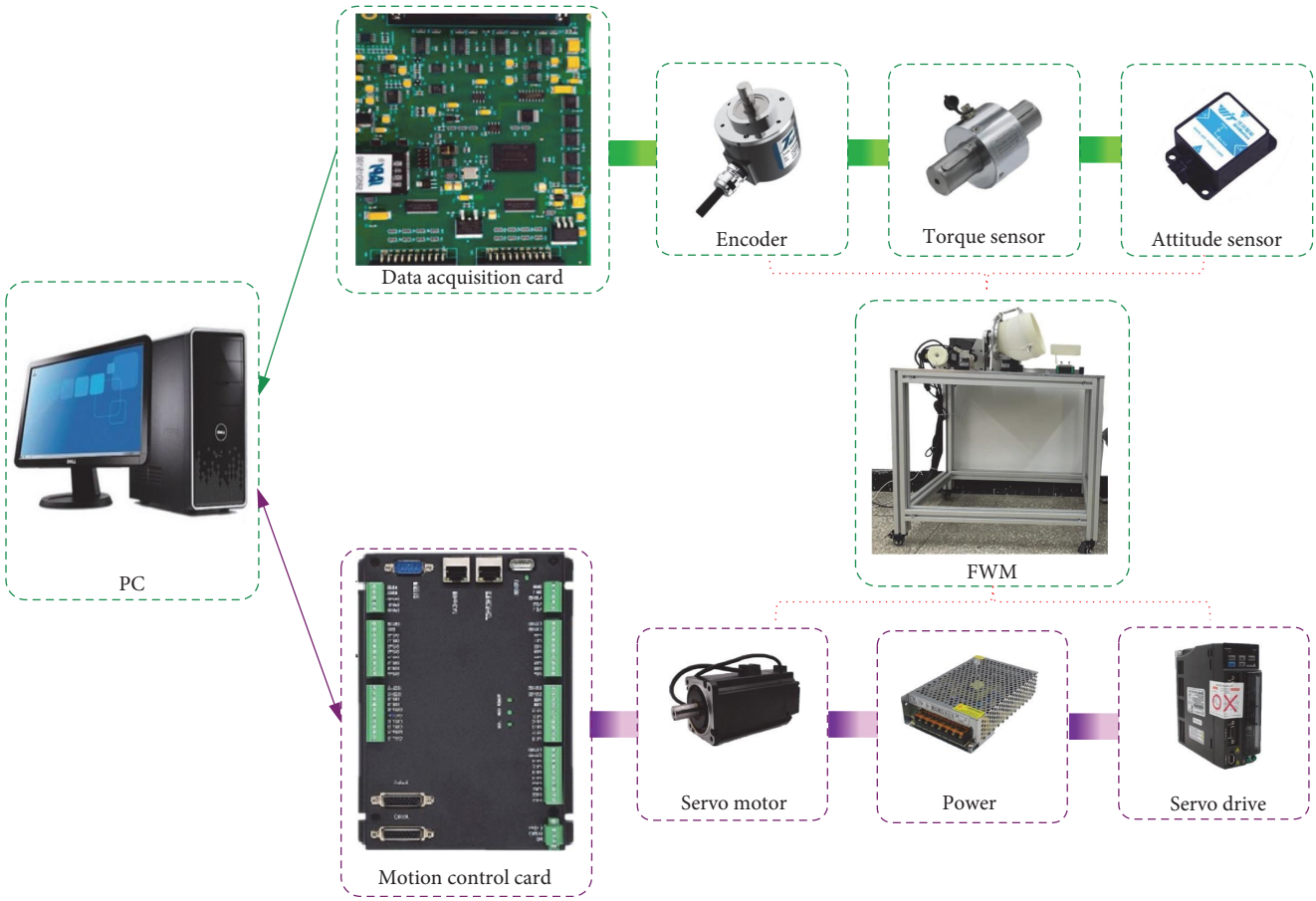

Figure 11: Diagram control system of FWM.

moving platform and the change of cables' length is shown in Figure 8.

From Figure 8, the length of cable is 0.1044 m in the initial position, when the moving platform moves around θ, i.e., the R/U deviation movement of the wrist joint, and the length of l_2 keeps the original length unchanged. The angle change of the moving platform is controlled by changing the length of l_1 and l_3. When the length of l_1 is shortened and l_3 is extended, the mechanism performs a radial flexion movement, and when the length of l_1 is extended and l_3 is shortened, the ulnar deviation movement is performed, conversely. When the moving platform moves around ϕ, i.e., the extension and flexion movement of the wrist joint and the length of l_1 and l_3 are equal. When the length of l_2 is shortened and l_1 and l_3 are extended, the mechanism performs an extension movement, and when the length of l_2 is extended and l_1 and l_3 are shortened, the flexion movement is performed.

For a rehabilitation mechanism, it is necessary to ensure that the moving platform satisfies the range of motion (ROM) of the forearm and wrist of the human body; the workspace of the calculation mechanism is required. According to the characteristics of the mechanism, the workspace of the mechanism can be described by position workspace and defined as the collection of the points of moving platform when cables are in tension.

As the cable has the property of providing tension force, when the plane of the moving platform and the cable are collinear, the limit position of the workspace is reached as shown in Figure 9. $B_1O_BB_3$ and $A_1O_AA_3$ are the moving platform and fixed platform, respectively. θ is the angle with which moving platform rotates around point O_B. θ gets the maximum value when B_1 rotates around O_B to B_1', and B_3 rotates to B_3', that is, points B_1', O_B, B_3', and A_3 are collinear at that time. The value of θ can be calculated as follows:

$$\theta = \arctan(h/r), \tag{18}$$

where h is the distance between points O_A and O_B. R and r are the radii of moving platform and fixed platform, respectively.

The volume of the workspace of the mechanism will increase with the increase of value of h/r. Figure 10 illustrates the workspace analysis of the mechanism with $r = 0.065$ m, $R = 0.095$ m, and $h = 0.1$ m. As shown in Figure 10, the value of workspace on Z-axis varies in a range of $(-8.227,\ 8.227\,\text{cm})$, and X- and Y-axis vary in a range of $(-9.5, 9.5\,\text{cm})$, and θ gets a maximum value of 119.946°. The workspace analysis results show that the mechanism

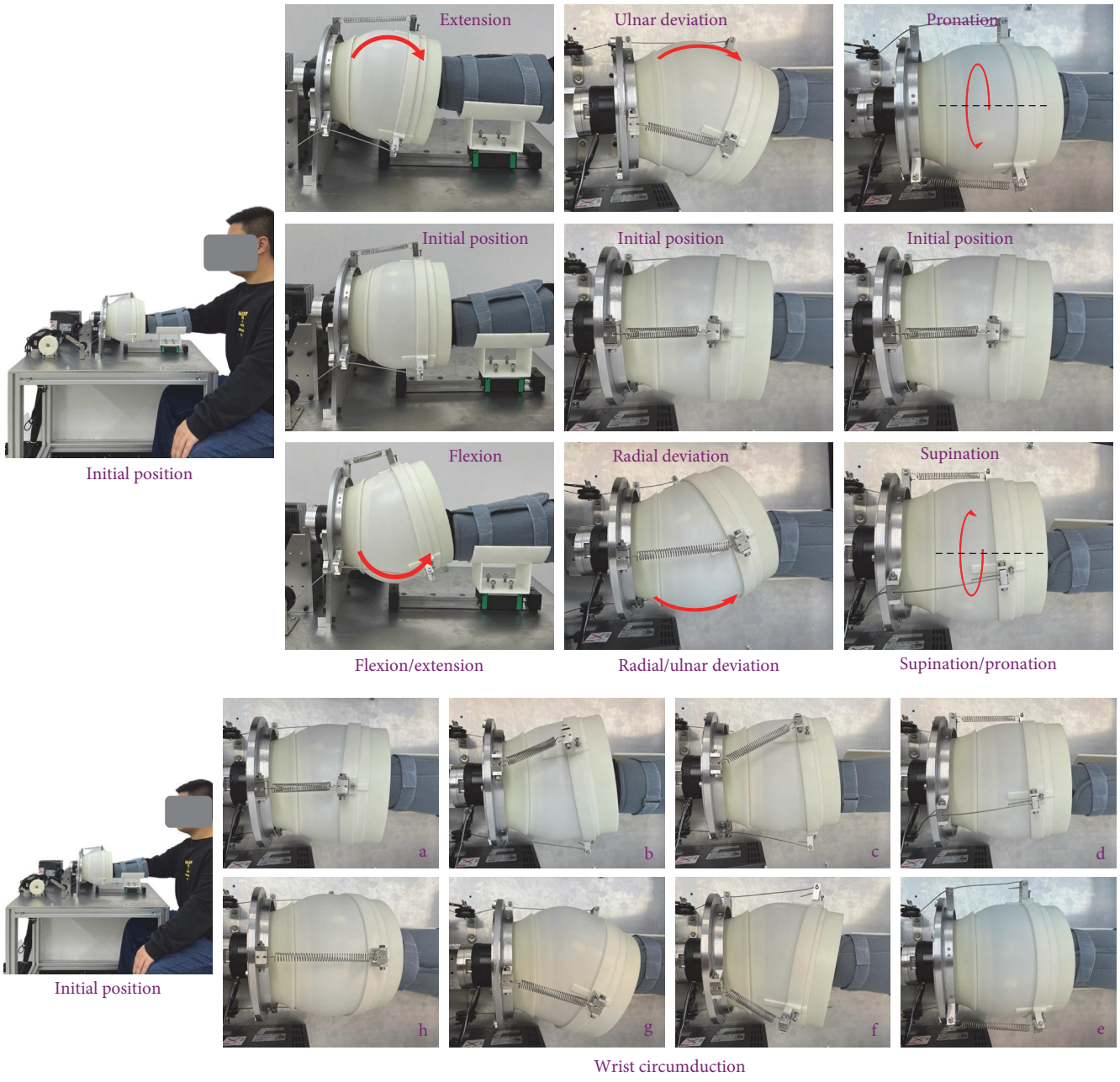

Figure 12: The movement of the FWM by the participant actively.

presented in this paper satisfies the joint mobility of the wrist joint.

4. Experiment

A prototype of the mechanism has been built, and the diagram control system of the FWM is shown in Figure 11. The sensors collect the motion data to transmit the computer by the data acquisition card, and the data are converted into motion parameters to transmit each servo drive by the motion control card. When using the device for rehabilitation training, the participant's forearm is placed on the forearm support frame, and the participant's hand is held or attached to the handle. The participant is required to wear a forearm brace to improve the comfort. FWM is suitable for bimanual rehabilitation without changing the mechanism. An emergency stop button is designed into the device to shut down the system's power in an emergency.

Figure 12 shows the movement of the FWM by the testing persons during autonomic movements. The active exercise is performed manually by the device which assists the participant's autonomous movement. The experiments show that the participant does forearm and wrist rehabilitation exercises actively by the mechanism. According to the experiment, the joint angle and speed can be measured during the acquisition. Measuring the joint angle and speed of the FWM

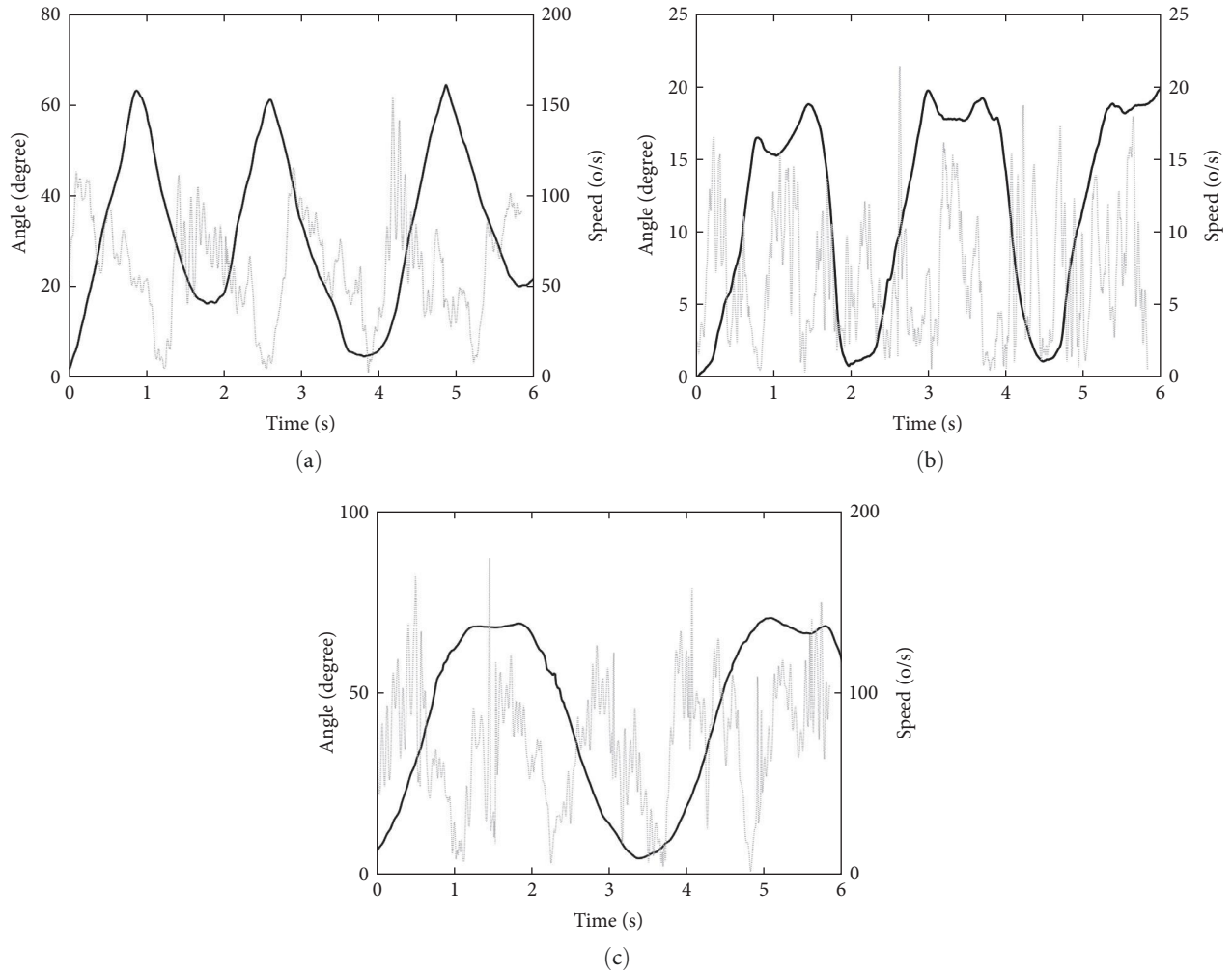

Figure 13: The joint angle and speed of the FWM. (a) F/E. (b) R/U deviation. (c) S/P.

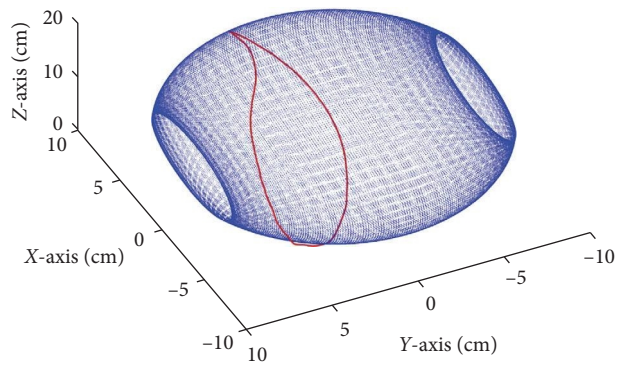

Figure 14: The trajectory of the circumduction.

is the same as the method used to test the PMS of forearm and wrist in Section 2. One participant, a healthy female, 25 years old, 175 cm, 75 kg, was asked to use FWM and perform several joint rotations at different speeds for each of the three movements. Figure 13 shows the data obtained at this stage.

When the FWM does the movement of circumduction by the participant, an elliptical curve will be obtained. The red curve in Figure 14 is the trajectory of the circumduction motion completed by the wrist using the device. The workspace of FWM contains circular trajectory, proving that the designed device can perform the motion of the human wrist.

As a rehabilitation mechanism, in addition to being able to complete passive movements, it is also important to be able to perform active movements. Figure 15 shows the angle

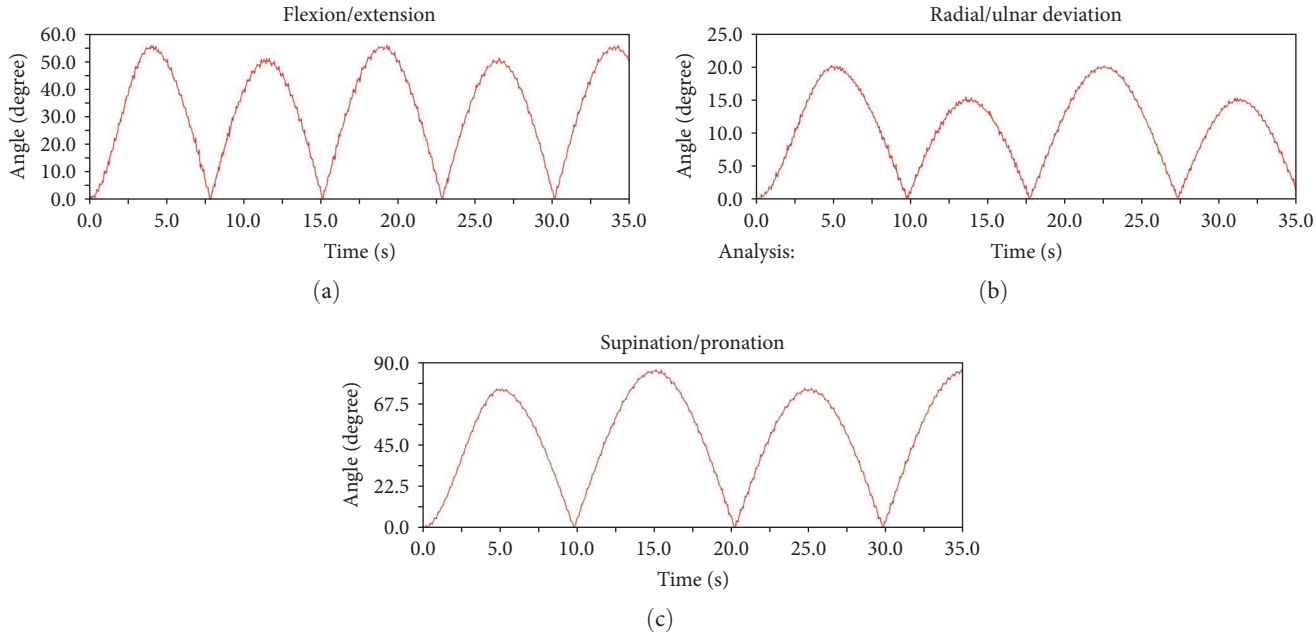

Figure 15: The angle of the movement of the FWM actively. (a) F/E. (b) R/U deviation. (c) S/P.

of the movement of the FWM in F/E, R/U deviation, and S/P, actively. Results indicated the joint ROM of the mechanism satisfies the PMS of the forearm and wrist joint, and the mechanism proposed in this paper can satisfy the requirements of the compound movements of the forearm and wrist. Therefore, the FWM has clinical significance and practical application value for the forearm and wrist rehabilitation. The experiments show that the mechanism proposed in this paper can complete the S/P of the forearm, R/U deviation, F/E, and circumduction of the wrist which cover the whole workspace of the forearm–wrist.

5. Conclusion

In this paper, first, an FWM is proposed for bilateral rehabilitation. The FWM not only satisfies the motion of a single joint with a single DoF but also can complete the wrist circumduction. The work focuses on the design of parallel mechanism, and the contributions are summarized as follows: (1) adding a spring solves the problem of cable slack. (2) A method is given to address the pose and force between the moving platform and cables in a parallel mechanism. (3) An actuator is decreased without changing the mobility, which can reduce the cost and weight of parallel mechanism. Then, mobility analysis has derived that the mechanism has three rotational DOFs satisfied the joint mobility of the forearm and wrist joint by screw theory. Significantly, to support the entire structure, a hemispherical shell is designed. At the same time, inverse kinematics, statics, the Jacobian matrix, and workspace of the mechanism are analyzed and derived. A prototype of the mechanism has been built to evaluate the capabilities of the mechanism during participants' tests. The obtained results have shown that the workspace of the mechanism covered the PMS of the forearm and wrist joint. The validity of the mechanism is expounded by covered the PMS of the forearm and wrist joint.

Data Availability

The datasets analyzed in this article are not publicly available. Requests to access the datasets should be directed to the corresponding author.

Conflicts of Interest

The authors declare that they have no conflicts of interest.

Funding

This research was funded by the National Natural Science Foundation of China, grant number 51875047 and the Foundation of Jilin Provincial Science and Technology, grant number 20220204102YY.

References

[1] C. W. Tsao, A. W. Aday, Z. I. Almarzooq et al., "Heart disease and stroke statistics—2022 update: a report from the American Heart Association," *Circulation*, vol. 145, no. 8, pp. e153–e639, 2022.

[2] M. R. Yochelson, A. C. Dennison, and A. L. Kolarova, "Stroke rehabilitation," in *Braddom's Physical Medicine and Rehabilitation*, D. X. Cifu, Ed., pp. 954–971, Elsevier, 6th edition, 2021.

[3] J. Bernhardt, E. Godecke, L. Johnson, and P. Langhorne, "Early rehabilitation after stroke," *Current Opinion in Neurology*, vol. 30, no. 1, pp. 48–54, 2017.

[4] N. Shimamura, T. Katagai, K. Kakuta et al., "Rehabilitation and the neural network after stroke," *Translational Stroke Research*, vol. 8, pp. 507–514, 2017.

[5] P. Zhao, Y. Zhang, H. Guan, X. Deng, and H. Chen, "Design of a single-degree-of-freedom immersive rehabilitation device for

clustered upper-limb motion," *Journal of Mechanisms and Robotics*, vol. 13, no. 3, Article ID 031006, 2021.

[6] Y. Mao and S. K. Agrawal, "Design of a cable-driven arm exoskeleton (CAREX) for neural rehabilitation," *IEEE Transactions on Robotics*, vol. 28, no. 4, pp. 922–931, 2012.

[7] Y. Mao, X. Jin, G. G. Dutta, J. P. Scholz, and S. K. Agrawal, "Human movement training with a cable driven ARm EXoskeleton (CAREX)," *IEEE Transactions on Neural Systems and Rehabilitation Engineering*, vol. 23, no. 1, pp. 84–92, 2015.

[8] D. J. Reinkensmeyer, L. E. Kahn, M. Averbuch, A. McKenna-Cole, B. D. Schmit, and W. Z. Rymer, "Understanding and treating arm movement impairment after chronic brain injury: progress with the ARM guide," *Journal of Rehabilitation Research and Development*, vol. 37, no. 6, pp. 653–662, 2000.

[9] P. S. Lum, C. G. Burgar, and P. C. Shor, "Evidence for improved muscle activation patterns after retraining of reaching movements with the MIME robotic system in subjects with post-stroke hemiparesis," *IEEE Transactions on Neural Systems and Rehabilitation Engineering*, vol. 12, no. 2, pp. 186–194, 2004.

[10] R. J. Sanchez, J. Liu, S. Rao et al., "Automating arm movement training following severe stroke: functional exercises with quantitative feedback in a gravity-reduced environment," *IEEE Transactions on Neural Systems and Rehabilitation Engineering*, vol. 14, no. 3, pp. 378–389, 2006.

[11] P. J. Mansfield and D. A. Neumann, *Essentials of Kinesiology for the Physical Therapist Assistant*, Elsevier, Missouri, 3rd edition, 2018.

[12] Z. Kadivar, J. L. Sullivan, D. P. Eng et al., "RiceWrist robotic device for upper limb training: feasibility study and case report of two tetraplegic persons with spinal cord injury," *International Journal of Biological Engineering*, vol. 2, no. 4, pp. 27–38, 2012.

[13] A. U. Pehlivan, C. Rose, and M. K. O'Malley, "System characterization of RiceWrist-S: a forearm–wrist exoskeleton for upper extremity rehabilitation," in *2013 IEEE 13th International Conference on Rehabilitation Robotics (ICORR)*, pp. 1–6, IEEE, Seattle, WA, USA, June 2013.

[14] K. D. Fitle, A. U. Pehlivan, and M. K. O'Malley, "A robotic exoskeleton for rehabilitation and assessment of the upper limb following incomplete spinal cord injury," in *2015 IEEE International Conference on Robotics and Automation (ICRA)*, pp. 4960–4966, IEEE, Seattle, WA, USA, 2015.

[15] A. Gupta and M. K. O'Malley, "Design of a haptic arm exoskeleton for training and rehabilitation," *IEEE/ASME Transactions on Mechatronics*, vol. 11, no. 3, pp. 280–289, 2006.

[16] D. Buongiorno, E. Sotgiu, D. Leonardis, S. Marcheschi, M. Solazzi, and A. Frisoli, "WRES: a novel 3 DoF WRist ExoSkeleton with tendon-driven differential transmission for neuro-rehabilitation and teleoperation," *IEEE Robotics and Automation Letters*, vol. 3, no. 3, pp. 2152–2159, 2018.

[17] Z. Pang, T. Wang, J. Yu, S. Liu, X. Zhang, and D. Jiang, "Design and analysis of a flexible, elastic, and rope-driven parallel mechanism for wrist rehabilitation," *Applied Bionics and Biomechanics*, vol. 2020, Article ID 8841400, 13 pages, 2020.

[18] N. Dunkelberger, J. Berning, K. J. Dix, S. A. Ramirez, and M. K. O'Malley, "Design, characterization, and dynamic simulation of the MAHI open exoskeleton upper limb robot," *IEEE/ASME Transactions on Mechatronics*, vol. 27, no. 4, pp. 1829–1836, 2022.

[19] A. Rastegarpanah, M. Saadat, and A. Borboni, "Parallel robot for lower limb rehabilitation exercises," *Applied Bionics and Biomechanics*, vol. 2016, Article ID 8584735, 10 pages, 2016.

[20] D. Cafolla, M. Russo, and G. Carbone, "CUBE, a cable-driven device for limb rehabilitation," *Journal of Bionic Engineering*, vol. 16, pp. 492–502, 2019.

[21] B. Gao, H. Song, J. Zhao, S. Guo, L. Sun, and Y. Tang, "Inverse kinematics and workspace analysis of a cable-driven parallel robot with a spring spine," *Mechanism and Machine Theory*, vol. 76, pp. 56–69, 2014.

[22] J. Ueda, D. Ming, V. Krishnamoorthy, M. Shinohara, and T. Ogasawara, "Individual muscle control using an exoskeleton robot for muscle function testing," *IEEE Transactions on Neural Systems and Rehabilitation Engineering*, vol. 18, no. 4, pp. 339–350, 2010.

[23] L. Zhang, J. Li, Y. Cui, M. Dong, B. Fang, and P. Zhang, "Design and performance analysis of a parallel wrist rehabilitation robot (PWRR)," *Robotics and Autonomous Systems*, vol. 125, Article ID 103390, 2020.

[24] C. A. Nelson, L. Nouaille, and G. Poisson, "A redundant rehabilitation robot with a variable stiffness mechanism," *Mechanism and Machine Theory*, vol. 150, Article ID 103862, 2020.